

Toward rapid and inexpensive identification of bulk carbon nanotubes

K. E. H. Gilbert and J. H. Lehman^{a)}

National Institute of Standards and Technology, Boulder, Colorado 80305

A. C. Dillon and J. L. Blackburn

National Renewable Energy Laboratory, Golden, Colorado 80401

(Received 14 December 2005; accepted 26 February 2006; published online 6 April 2006)

The volume fraction of metallic and semiconducting carbon single-wall nanotubes (SWNTs) has been estimated for purified laser vaporization SWNTs, from an effective medium approximation and the measured spectral responsivity of a LiTaO₃ pyroelectric detector covered with SWNT “bucky” paper. The detector spectral responsivity from 600 to 2000 nm is proportional to the expected absorption coefficient of the SWNTs, and variations near 700, 950, and 1750 nm correlate with characteristic interband transitions and proportions of SWNTs consistent with 20% metal and 80% semiconductor materials. © 2006 American Institute of Physics. [DOI: 10.1063/1.2193797]

The optical properties of bulk single-wall carbon nanotubes (SWNTs) have been studied by a variety of means including near-infrared spectroscopy, Raman spectroscopy, and photoluminescence.¹ We are pursuing techniques for rapid and inexpensive identification of bulk carbon nanotubes to facilitate commercialization as well as to advance our own interest in developing improved thermal detector coatings. The method we present is that of applying SWNTs to a pyroelectric detector, measuring their spectral responsivity, and estimating the volume fraction of metallic and semiconducting SWNTs with an effective medium approximation (EMA).^{2,3} Our EMA analysis relies on previous work by Ugawa *et al.*⁴ and Chen⁵ with consideration of purity studies by Dillon *et al.*,⁶ Itkis *et al.*,⁷ and Landi *et al.*⁸

Despite the visibly black appearance of bulk SWNTs, their dielectric properties yield variations in absorption coefficient. This is due to features such as chirality, diameter, purity, and bulk topology.⁸ By measuring the detector responsivity, we take advantage of a relatively large specular absorptance at normal incidence, which is easily modeled from simplified Fresnel equations for normal incidence. This is an advantage over that of determining optical properties by measuring a small diffuse reflectance or transmittance of SWNTs in solution. Arguably, evaluation of SWNTs is less repeatable over time if the SWNTs fall out of suspension.⁹ SWNTs on a fixed platform such as a pyroelectric detector are repeatable over time and are compatible with other important measurement techniques such as Raman spectroscopy.

The SWNTs were synthesized by a laser vaporization method similar to that reported previously.¹⁰ Here, however, an Alexandrite laser operating at a wavelength of 755 nm was employed to vaporize a graphite target doped with cobalt and nickel (each at 0.6% relative atomic mass). The crude soot was produced at 1175 °C with 500 torr argon flowing at 100 cm³/min. The average laser power density was 55 W/cm² with an elliptical spot size, approximately 1.84 × 0.8 mm². The SWNTs were purified by oxidation of the soot in flowing CO₂ at 800 °C for 1 h, followed by a reflux in 3 M HNO₃ for 16 h. The solution was then filtered,

washed, and dried at 50 °C for 30 min. During this drying process the SWNTs separated from the filter, producing a free standing “bucky” paper. The paper was further oxidized in air at 550 °C for 30 min as described previously.⁶ The material purity was greater than 97% by weight as determined by thermogravimetric analysis.¹¹ Additionally, Raman spectroscopy with laser excitation (E_{laser}) at 2.54 eV was employed to analyze the disorder induced *D* band at ~ 1350 cm⁻¹. The full width at half maximum (FWHM) of the *D* band was ~ 18.7 cm⁻¹, and the *D/G* ratio was 0.0075. The frequencies of the radial breathing modes indicated that the resonant diameter distribution was in the range of 1.3–1.5 nm. Therefore, the FWHM of the *D* band for the purified sample is consistent with material that is virtually free of non-nanotube carbon impurities.¹² Raman spectra taken with $E_{\text{laser}}=1.96$ eV indicated a broader resonant diameter range of approximately 1.2–1.7 nm. The spectra acquired with these two separate excitation energies indicated the presence of both semiconducting and metallic tubes.

The pyroelectric detector to which the SWNTs were applied was prepared from a *z*-cut LiTaO₃ plate 12 mm in diameter and 60 μm thick. The electrode centered on the back side of the LiTaO₃ plate was 10 mm in diameter and consisted of 50 nm of gold on top of 25 nm of chromium. The front electrode, to which the SWNTs were applied, was 25 nm of chromium. The back electrode was connected to the signal input of a current amplifier with 10⁻¹⁰ A/V gain, and the front electrode was connected to ground. The optical input to the detector was modulated at 15 Hz and measured with a lock-in detection scheme.¹³ A sample of bucky paper, approximately 5 × 5 mm², was placed on the front with a drop of chloroform to facilitate adhesion. The paper then remained attached to the detector after the chloroform evaporated.

The measurement system for the spectral responsivity consists of a lamp source, a grating monochromator, and a NIST transfer-standard detector as shown in Fig. 1.³ The method of direct substitution provides absolute spectral responsivity relative to the NIST standard at 10 nm wavelength increments from 600 to 2000 nm with a relative expanded uncertainty of 1.24%. For this work, the beam exiting the monochromator was focused on the bucky paper to a beam size of approximately 2 × 2 mm², normal to the

^{a)} Author to whom correspondence should be addressed; electronic mail: lehman@boulder.nist.gov

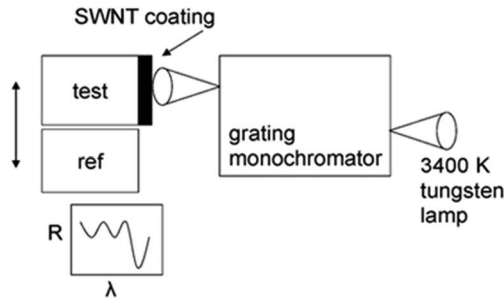


FIG. 1. Schematic diagram of the lamp and monochromator based measurement systems.

plane of the detector surface, with a bandwidth of 6 nm.

The current generated by a pyroelectric detector is proportional to the volume average of the change in temperature as a function of time. Its spectral responsivity depends only on conversion of optical energy to thermal energy by the coating. Thus, the spectral responsivity of a pyroelectric detector coated with purified nanotubes can reveal optical properties of the coating from the ultraviolet to far into the infrared spectrum. The spectral responsivity measurement results shown in Fig. 2 for the SWNT coated detector are distinguished by variations in relative responsivity for the wavelength range between 600 and 2000 nm. Specifically, three broad dips are observed at approximately 1.789, 1.240, and 0.690 eV, corresponding to characteristic ${}^M E_{11}$, ${}^S E_{22}$, and ${}^S E_{11}$ interband transitions, respectively.⁷

An EMA has been employed in the past to calculate a dielectric function of bulk SWNTs containing a mixture of metallic and semiconducting SWNTs.⁴ In our previous work, we neglected interband transitions and, rather than fitting our data to the model merely proposed that an EMA might be sufficient to quantify the proportion of metallic and semiconducting nanotubes. The present analysis goes further by fitting our measurement results and estimating the proportions of metallic and semiconducting SWNTs. We restate the EMA equation from Ugawa *et al.*,⁴

$$f \frac{\varepsilon_m(\omega) - \varepsilon(\omega)}{g\varepsilon_m(\omega) + (1-g)\varepsilon(\omega)} + (1-f) \frac{\varepsilon_s(\omega) - \varepsilon(\omega)}{g\varepsilon_s(\omega) + (1-g)\varepsilon(\omega)} = 0, \quad (1)$$

where the fill factor f is the dominant fit parameter for the volume fraction of semiconducting to metallic SWNTs. The value of the depolarization factor g has not been addressed in detail for SWNTs. Indeed, calculation of the EMA [Eq. (1)] neglecting the depolarization factor appears to be insignificant for values of g between 0.01 and 0.1. The solution of Eq. (1) for the effective dielectric function $\varepsilon(\omega)$ is a quadratic form, but reduces to a weighted average based on the value of f if g is neglected. For our application, f is the sole fit parameter with which we estimate the volume fraction of tube type.

Ugawa *et al.*⁴ and separately Chen⁵ base Eq. (1) on two dielectric functions: a Drude model for metallic SWNTs,

$$\varepsilon_m(\omega) = \varepsilon_\infty - \frac{\omega_p^2}{\omega^2 + i\gamma\omega} - \frac{\Omega_1^2}{\omega^2 - \omega_1^2 + i\Gamma_1\omega}, \quad (2)$$

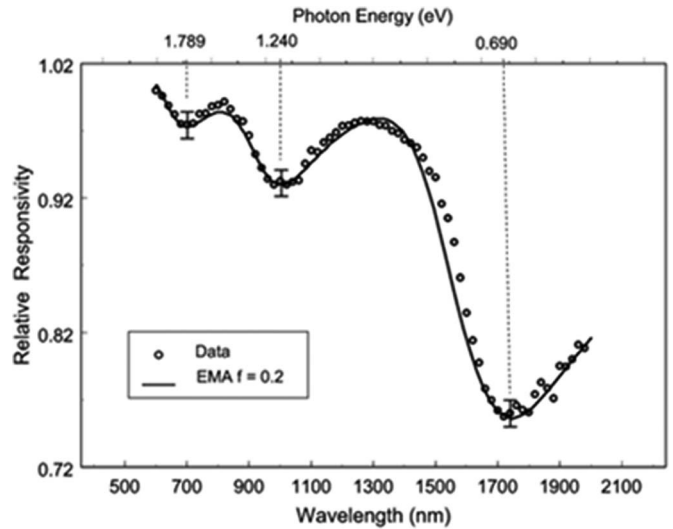


FIG. 2. Measured detector responsivity and calculated expected responsivity for purified laser-generated SWNTs. The relative expanded uncertainty of the measured values is 1.24%, as shown in three typical error bars. The level of confidence for the uncertainty is approximately 95%.

and a Lorentzian model for semiconducting SWNTs,

$$\varepsilon_s(\omega) = \varepsilon_\infty - \frac{\Omega_2^2}{\omega^2 - \omega_2^2 + i\Gamma_2\omega} - \frac{\Omega_3^2}{\omega^2 - \omega_3^2 + i\Gamma_3\omega}, \quad (3)$$

where ε_∞ is the electronic core contribution, ω_p is the plasma frequency of charge carriers, ω_n is the center frequency, ω is the photon frequency, and γ , Ω_n , and Γ_n are the relative relaxation rates of the charge carriers of the metal and semiconductor interband transitions, ${}^M E_{11}$ ($n=1$), ${}^S E_{11}$ ($n=2$), and ${}^S E_{22}$ ($n=3$), respectively. The following parameters were used for the combined models: $\varepsilon_\infty=1.732$ eV/ \hbar , $\omega_p=0.441$ eV/ \hbar , $\gamma=0.188$ eV/ \hbar , $\Gamma_1=0.520$ eV/ \hbar , $\Gamma_2=0.163$ eV/ \hbar , $\Gamma_3=0.345$ eV/ \hbar , $\omega_1=1.789$ eV/ \hbar , $\omega_2=0.690$ eV/ \hbar , $\omega_3=1.240$ eV/ \hbar , $\Omega_1=2.011$ eV/ \hbar , $\Omega_2=0.845$ eV/ \hbar , $\Omega_3=0.875$ eV/ \hbar , $g=0.01$. These values are similar to those given by Chen⁵ which were determined iteratively by means of the Kramers-Kronig relations, and are given with the caution that the fit is more likely to fall within our measurement uncertainty for the interband between 0.6 and 2 eV. The physical significance of these parameters is discussed in greater detail by both Ugawa *et al.*⁴ and Chen.⁵

The absorption coefficient $\alpha(\omega)$ of the detector coating was calculated from the Fresnel equations for light incident on the detector at normal incidence, with the index determined from the real and imaginary roots of $\varepsilon(\omega)$. The solution for $f=0.2$ is plotted on the basis of optical wavelength for comparison with the measured data in Fig. 2. The experiment and model agree to within the measurement uncertainty of the experimental data over the range of 600–2000 nm except for data points at 1550 and 1600 nm. Further analysis of $\alpha(\omega)$ where the responsivity is changing dramatically in this region reveals that a change in responsivity as small as 4% is manifested by a change in ratio of metallic:semiconducting SWNTs of approximately 10%. Hence, a routine spectral responsivity calibration of a SWNT-coated pyroelectric detector is adequate to estimate the ratio of metallic:semiconducting composition at the 10% level.

The variation in *shape* of the responsivity is most relevant to reconciling the EMA with the optical properties of the SWNT coating. However, the *magnitude* of the respon-

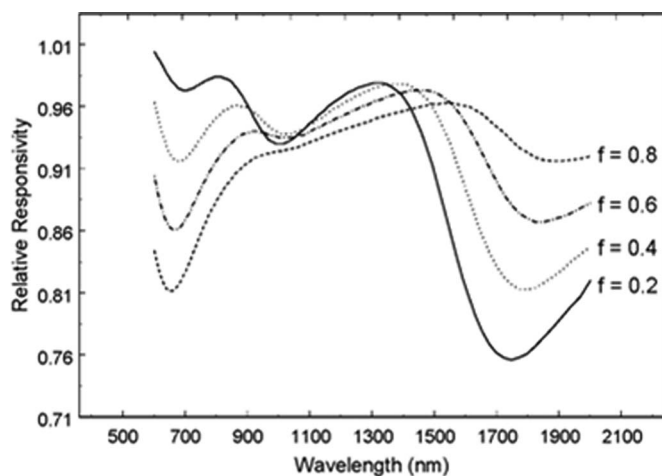


FIG. 3. Calculated values of detector responsivity depending on the fill factor of the SWNT coating, where $f=1$ is exclusively metallic and $f=0$ is semiconducting.

sivity can depend on the thickness of the coating, the thermal contact between the coating and the detector electrodes, or the topology of the SWNTs in the paper form. Compared to an identical detector having a coating with greater than 99% absorption efficiency, the absorption coefficient for the bucky paper studied here is 67% at 600 nm. Further investigation is required to understand the significance of thickness, topology, and thermal contact in relation to the responsivity.

The ease of measurement and analysis, if considered along with economic factors, suggest our technique may be considered a rapid and inexpensive compliment to other important tools for SWNT metrology. Presently the EMA approach is among the only means of estimating the volume fraction of metallic and semiconducting SWNTs. For example, Raman spectroscopy will confirm the *presence* of both metallic and semiconducting SWNTs; however, quantitative characterization is extremely difficult. The work of Landi *et al.*⁸ convincingly shows the influence of impurities on spectral absorption. So far we believe our approach is valid for measurements near the $^M E_{11}$, $^S E_{11}$, and $^S E_{11}$ interband transitions for pure SWNTs. In Fig. 3 we show example calculations for volume fractions other than what we have

measured. The results depict the expected variation of the detector responsivity for a bulk composition ranging from 20% metal content ($f=0.2$) to 80% ($f=0.8$). This will be validated as chirality specific production processes are developed and enriched samples become available for us to evaluate.

Our measurements of purified SWNTs produced by laser vaporization and applied to a pyroelectric detector have sufficient length and lack of defects to exhibit a spectral character in the wavelength range of 600–2000 nm to reveal interband transitions that are characteristic of either metallic or semiconducting SWNTs. The sample we have evaluated by means of spectral responsivity and EMA indicates that such SWNTs produced by laser (755 nm) vaporization at 55 W/cm² have a proportion of SWNT material content that is 20% metallic and 80% semiconducting. Furthermore, we have presented a model to estimate the relative concentration of metallic to semiconducting SWNTs applicable for highly pure samples.

The authors gratefully acknowledge M. J. Heben for helpful discussions and the use of materials from NREL.

¹S. M. Bachilo, M. S. Strano, C. Kittrell, R. H. Hauge, R. E. Smalley, and R. B. Weisman, *Science* **298**, 2361 (2002).

²J. H. Lehman, C. Engtrakul, T. Gennett, and A. C. Dillon, *Appl. Opt.* **44**, 483 (2004).

³J. H. Lehman, NIST Spec. Publ. **250-53**, 1 (1999).

⁴A. Ugawa, A. G. Rinzler, and D. B. Tanner, *Phys. Rev. B* **60**, R11305 (1999).

⁵G. Chen, Ph.D. dissertation, Pennsylvania State University, 2003.

⁶A. C. Dillon, T. Gennett, K. M. Jones, J. L. Alleman, P. A. Parilla, and M. J. Heben, *Adv. Mater. (Weinheim, Ger.)* **11**, 1354 (1999).

⁷M. E. Itkis, D. E. Perea, S. Niyogi, S. M. Rickard, M. A. Hamon, H. Hu, B. Zhao, and R. C. Haddon, *Nano Lett.* **3**, 3 309 (2003).

⁸B. J. Landi, H. J. Ruf, C. M. Evans, C. D. Cress, and R. P. Raffaele, *J. Phys. Chem. B* **109**, 9952 (2005).

⁹V. C. Moore, M. S. Strano, E. H. Haroz, R. H. Hauge, and R. E. Smalley, *Nano Lett.* **3**, 1379 (2003).

¹⁰A. C. Dillon, P. A. Parilla, J. L. Alleman, J. D. Perkins, and M. J. Heben, *Chem. Phys. Lett.* **316**, 13 (2000)

¹¹K. E. H. Gilbert, Ph.D. Dissertation, Colorado School of Mines, 2005.

¹²A. C. Dillon, M. Yudasaka, and M. S. Dresselhaus, *J. Nanosci. Nanotechnol.* **4**, 691 (2004).

¹³J. H. Lehman, G. Eppeldauer, J. A. Aust, and M. Racz, *Appl. Opt.* **38**, 7047 (1999).